Journal of the American College of Cardiology Vol. 60, No. 21, 2012

Published by Elsevier Inc.
ISSN 0735-1097/$36.00
http://dx.doi.org/10.1016/j.jacc.2012.07.053

In Silico Cardiac Risk Assessment in Patients With Long QT Syndrome

Type 1: Clinical Predictability of Cardiac Models

Ryan Hoefen, MD, PhD,* Matthias Reumann, PhD,† Ilan Goldenberg, MD,* Arthur J. Moss, MD,* Jin O-Uchi, MD, PhD,‡ Yiping Gu, PhD,§ Scott McNitt, MS,* Wojciech Zareba, MD, PhD,* Christian Jons, MD,* Jorgen K. Kanters, MD,‖ Pyotr G. Platonov, MD, PhD,¶ Wataru Shimizu, MD,# Arthur A. M. Wilde, MD, PhD,** John Jeremy Rice, PhD,§ Coeli M. Lopes, PhD‡

Rochester, New York; Melbourne, Australia; Yorktown Heights, New York; Copenhagen, Denmark; Lund, Sweden; Suita, Japan; and Amsterdam, the Netherlands

Objectives The study was designed to assess the ability of computer-simulated electrocardiography parameters to predict clinical outcomes and to risk-stratify patients with long QT syndrome type 1 (LQT1).

Background Although attempts have been made to correlate mutation-specific ion channel dysfunction with patient phenotype in long QT syndrome, these have been largely unsuccessful. Systems-level computational models can be used to predict consequences of complex changes in channel function to the overall heart rhythm.

Methods A total of 633 LQT1-genotyped subjects with 34 mutations from multinational long QT syndrome registries were studied. Cellular electrophysiology function was determined for the mutations and introduced in a 1-dimensional transmural electrocardiography computer model. The mutation effect on transmural repolarization was determined for each mutation and related to the risk for cardiac events (syncope, aborted cardiac arrest, and sudden cardiac death) among patients.

Results Multivariate analysis showed that mutation-specific transmural repolarization prolongation (TRP) was associated with an increased risk for cardiac events (35% per 10-ms increment [$p < 0.0001$]; ≥upper quartile hazard ratio: 2.80 [$p < 0.0001$]) and life-threatening events (aborted cardiac arrest/sudden cardiac death: 27% per 10-ms increment [$p = 0.03$]; ≥upper quartile hazard ratio: 2.24 [$p = 0.002$]) independently of patients' individual QT interval corrected for heart rate (QTc). Subgroup analysis showed that among patients with mild to moderate QTc duration (<500 ms), the risk associated with TRP was maintained (36% per 10 ms [$p < 0.0001$]), whereas the patient's individual QTc was not associated with a significant risk increase after adjustment for TRP.

Conclusions These findings suggest that simulated repolarization can be used to predict clinical outcomes and to improve risk stratification in patients with LQT1, with a more pronounced effect among patients with a lower-range QTc, in whom a patient's individual QTc may provide less incremental prognostic information. (J Am Coll Cardiol 2012;60:2182–91) © 2012 by the American College of Cardiology Foundation

Long QT syndrome (LQTS) may cause torsade de pointes arrhythmia, ventricular fibrillation, and sudden cardiac death (SCD). The disease can either be inherited as a congenital ion channel mutation or acquired as a result of drugs that block these cardiac ion currents. Type 1 long QT syndrome (LQT1), the most common form of LQTS, is

From the *Division of Cardiology, Department of Medicine, University of Rochester School of Medicine and Dentistry, Rochester, New York; †IBM Research Collaboratory for Life Sciences, Melbourne, Australia; ‡Cardiovascular Research Institute, Department of Medicine, University of Rochester School of Medicine and Dentistry, Rochester, New York; §IBM Research Functional Genomics and Systems Biology, IBM T. J. Watson Research Center, Yorktown Heights, New York; ‖Gentofte University Hospital & University of Copenhagen, Copenhagen, Denmark; ¶Department of Cardiology, Lund University, Lund, Sweden; #National Cardiovascular Center, Suita, Japan; and the **Department of Clinical Genetics (NH), Academic Medical Centre, University of Amsterdam, Amsterdam, the Netherlands. Dr. Wilde is a member of the advisory board of Sorin and PGxHealth. Dr. Goldenberg has been a paid consultant for Boston Scientific. Dr. Jons reports receiving speaker's fees from Boehringer Ingelheim. All other authors have reported that they have no relationships relevant to the contents of this paper to disclose. Drs. Hoefen and Reumann are joint first authors; they contributed equally to this work. Drs. Lopes and Goldenberg are first authors for this paper.

Manuscript received January 7, 2012; revised manuscript received July 19, 2012, accepted July 23, 2012.

caused by loss-of-function mutations in the *KCNQ1* gene, which encodes the alpha subunit of the cardiac ion channel involved in the slow delayed rectifier potassium current (IKs) (1). To date, >300 different mutations have been identified in this gene (2).

See page 2192

The occurrence of cardiac events in patients with LQT1 is variable, with proper risk stratification needed to optimize patient treatment (3–6). Several phenotype variables have been associated with a more severe clinical course in patients with LQT1. QT interval corrected for heart rate (QTc) is one of the most effective risk stratifiers in LQTS, with previous studies showing a 4.2-fold risk increase in aborted cardiac arrest (ACA) or SCD among patients with a QTc ≥500 ms (4). However, QTc can vary temporally and among individuals with the same mutation (7). Mutation characteristics have recently been shown to determine cardiac risk in patients with genetically confirmed LQTS but normal-range QTc intervals (8–10). This suggests a strong genetic component to cardiac risk that is not currently understood.

Although several attempts have been made to correlate decrease in IKs function associated with specific mutations with patient phenotype, these attempts have been largely unsuccessful (8,11–13). Systems level computational models are highly developed in the field of cardiac physiology and can be used to predict consequences of complex changes in channel function to the overall heart rhythm. The authors hypothesized that: 1) mutation-specific transmural repolarization prolongation (TRP), obtained by simulating transmural electrocardiograms (ECGs) using a 1-dimensional (1D) cable model, will be an independent predictor of cardiac events among patients with LQT1; and 2) data regarding mutation-specific simulated TRP will identify increased risk for cardiac events among patients with LQT1 with mild to moderate QTc prolongation, in whom a patient's individual QTc provides less incremental prognostic information.

Methods

Simulation of pseudo-transmural ECGs with a 1D cable model. The 1D cable model of 192 cells was constructed and parameterized to represent the transmural heterogeneity across the ventricular wall. As shown in Figure 1A, each of the 192 cells was assigned varying properties based on its position within the ventricular wall. The cell model was adapted from the Flaim-Giles-McCulloch (FGM) reconstruction of the canine cardiac cell (14). The FGM model reconstructs 3 stereotyped cell types: epicardial (Epi), endocardial (Endo), and midmyocardial (M) cell responses. The FGM epicardial cell corresponds to the rightmost 30% of the wall in the cable model (70% to 100% wall distance in Online Fig. 1). The FGM endocardial cells correspond to the leftmost edge of the cable (0%), while the midmyocardial cell is mapped 10% wall depth in the subendocardium. For the present model, the profiles of conductance of late sodium current (I_{NaL}) and IKs were linearly interpolated between the different stereotyped cell types (Online Fig. 1). The model conduction velocity and action potential duration distributions are similar to experimental data (Online Fig. 2). The pseudo-transmural ECG was computed based on the transmural voltage gradient from the epicardial to the endocardial sides of the heart. In contrast to models in some published studies that report only a single electrode voltage located near the epicardium (15,16), the present model generates T waves sensitive to the whole transmural repolarization profile.

Abbreviations and Acronyms

ACA = aborted cardiac arrest
AP = action potential
ECG = electrocardiography
FGM = Flaim-Giles-McCulloch
IKs = rectifier potassium current
LQT1 = long QT syndrome type 1
LQTS = long QT syndrome
Q4 = upper quartile
QTc = QT interval corrected by heart rate
SCD = sudden cardiac death
TRP = transmural repolarization prolongation
WT = wild-type

Wild type (WT) IKs current parameters in the model were modified to mimic human IKs currents and currents measured for channels containing LQT1 mutant subunits previously reported by Jons et al (8). The first 5 cells are stimulated with applied current, and the action potential (AP) propagates to the end of the array. The AP propagates along an array of 288 cells, with the central 192 cells used in the analysis to circumvent edge artifacts (Online Fig. 3). The pacing protocol consists of 60 beats at a 1000-ms interval to bring the model to steady state. During the simulation studies, the modeling team was blinded to as which mutant corresponded to a given simulation (i.e., the modified parameters for the mutation were provided without a cross-reference to the mutation). For additional details on the in silico methods, see Online Appendix.

Study population data collection and clinical endpoints. The study population comprised 633 subjects derived from 103 LQT1 proband–identified families with genetically confirmed *KCNQ1* mutations for which mutant channel properties are known, permitting simulation with the method described here (see Online Table 1 for details of mutations included [8]). Patients were drawn from 3 LQTS registries—the U.S. part of the Rochester-based LQTS Registry (n = 488), the Japan-based LQTS Registry (n = 56), and the Netherlands-based LQTS Registry (n = 23)—as well as from data submitted by other investigators specifically for this collaborative mutation-analysis project (Denmark [n = 12] and Sweden [n = 4]). The proband in each family had diagnostic QTc prolongation and may or may not have experienced LQTS-related symptoms. Patients were excluded from the study if they had >1 LQTS-causing mutation (n = 9).

JACC Vol. 60, No. 21, 2012
November 20/27, 2012:2182–91

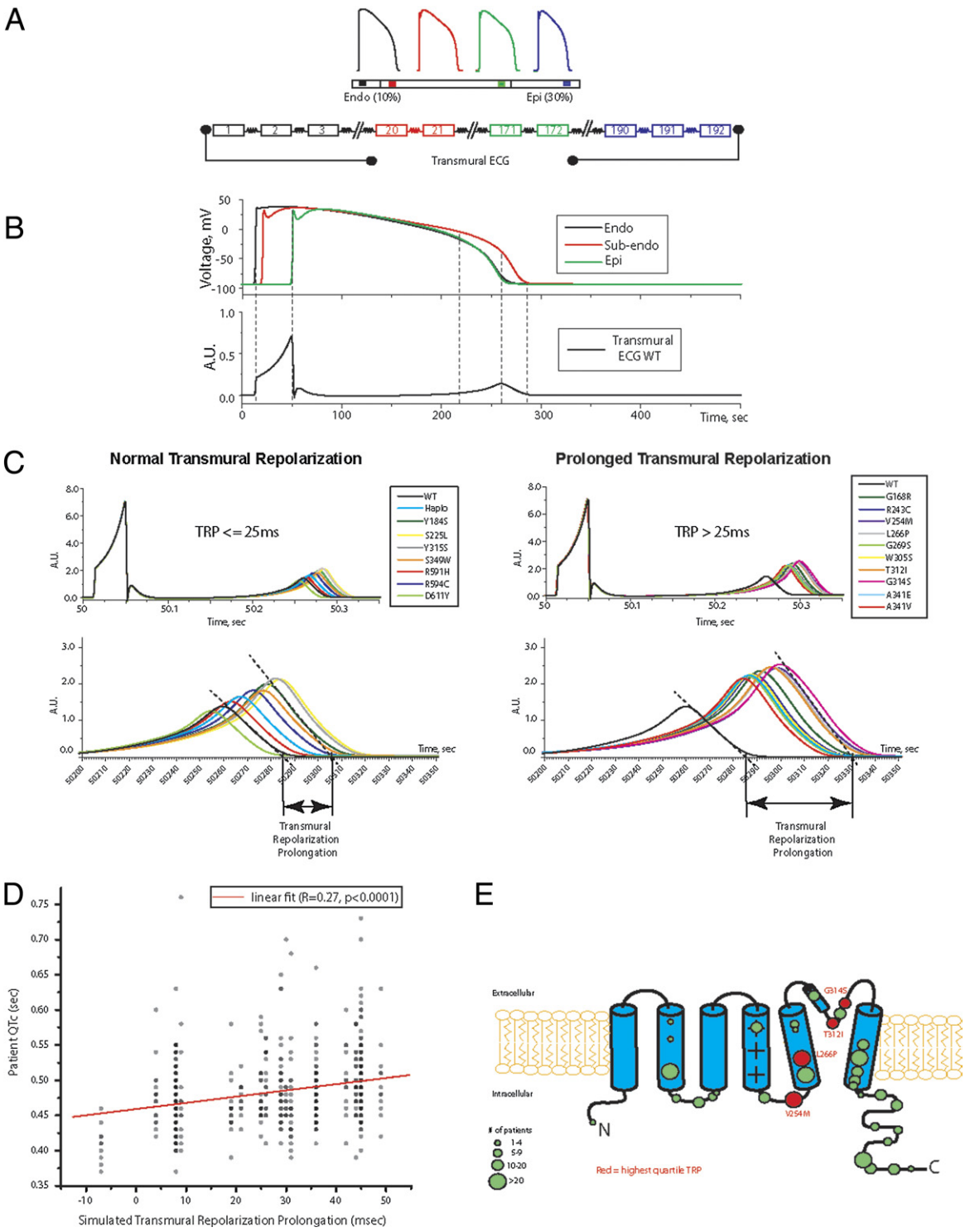

Figure 1 **Determination of TRP for Ion Channels Associated With LQT1**

(A) The 192-cell array used in the computational simulation of transmural repolarization prolongation (TRP) in patients with long QT syndrome type 1 (LQT1). Action potential determination for wild-type channels at the different cell types is shown. **(B)** Determination of pseudo-transmural electrocardiography (ECG) based on the wild-type channel action potential duration across the array of cells. **(C)** Pseudo-transmural ECG simulated for mutant channels in the study with lower **(left)** and higher **(right)** prolongation observed. A unique TRP parameter was determined for each mutant ion channel as indicated. **(D)** Correlation of TRP determined from simulation with patient QT interval corrected for heart rate (QTc) for all patients genotype positive for each mutation. **(E)** Location of mutations in the study. Mutations associated with the top quartile TRP are marked in **red.** **Circle size** indicates number of patients with the mutation.

Upon enrollment in the registry, clinical history was obtained; thus follow-up data in the current study comprised historical data from birth to enrollment and prospective information collected at yearly intervals after enrollment. The mean age at enrollment in the registry among the patients from the Rochester registry (77% of the patients studied) was 26 years, and follow-up for the survival analysis was from birth through age 40 years. On average, 69% of the follow-up data were obtained retrospectively at enrollment. Only patients for whom a complete medical history and prospective information were available were included in the present study. Clinical history data were collected on forms and included demographic characteristics, personal and family medical history, ECG findings, medical therapies, left cardiac sympathetic denervation, implantation of a pacemaker or an implantable cardioverter defibrillator (ICD), and the occurrence of LQTS-related cardiac events.

LQTS-related cardiac events included *syncope,* defined as transient loss of consciousness abrupt in onset and offset, ACA requiring defibrillation, and SCD without a known cause. Each subject had a single individual QTc value assigned, obtained at the time of entry in the LQT registry.

Genotyping. The *KCNQ1* mutations were identified with the use genetic tests performed in academic molecular-genetic laboratories, including the Functional Genomics Center, University of Rochester Medical Center, Rochester, New York; Baylor College of Medicine, Houston, Texas; Mayo Clinic College of Medicine, Rochester, Minnesota; Boston Children's Hospital, Boston, Massachusetts; Laboratory of Molecular Genetics, National Cardiovascular Center, Suita, Japan; Department of Clinical Genetics, Academic Medical Center, Amsterdam, The Netherlands; and Statens Serum Institut, Copenhagen, Denmark. For the proband in each family, the 5 most common LQT loci (*KCNQ1, KCNH2, SCN5A, KCNE1,* and *KCNE2*) were fully sequenced to identify the mutation by comparing the sequence with those of healthy individuals without LQTS. Once a mutation was identified in other family members, and the *KCNQ1* gene was sequenced to confirm the presence or absence of the mutation.

Specifically, after informed consent was obtained, blood samples from patients were sent for detailed mutational analysis involving either 12 LQTS genes (*KCNQ1, KCNH2, SCN5A, ANK2, KCNE1, KCNE2, CACNA1C, KCNJ2, CAV3, SCN4B, AKAP9,* and *SNTA1*) or 5 LQTS genes (*KCNQ1, KCNH2, SCN5A, KCNE1,* and *KCNE2*) and were screened for multiple LQTS mutations/polymorphisms. Genetic tests included next-generation DNA sequencing of all of the coding exons. For that, exons and adjacent splice sites of each of the genes were sequenced using a solid-state sequencing-by-synthesis process (Illumina, Inc., San Diego, California). There are over 230 exons to be sequenced in LQTS; 12 gene panels and both alleles of each exon (maternal and paternal) were sequenced simultaneously. Polymerase chain reaction primers flanking each exon of the regions of interest were designed to generate amplicons ranging in size from ~200 to 600 bp, avoiding any nonunique sequences, as well as positions of known polymorphisms and mutations. The products of all multiplex reactions for a specific patient were pooled. Sequencing itself first required cluster generation, which is the process of attaching individual fragments from a patient's library to a chambered glass slide and replicating them in situ to produce distinct islands of homogeneous fragments. Using the Genome Analyzer II (Illumina, Inc.), sequencing-by-synthesis chemistry was performed in the slide chambers to which the clusters were attached. Each base (A, C, G, or T) added to a growing DNA strand liberates 1 of 4 associated fluorochromes in a local reaction that was captured by photoimaging cycle for each cluster. Photoimaged data from each cluster of molecules were converted to base calls and aligned to a reference sequence for each gene of interest using Illumina-provided software. Various annotation databases (e.g., dbSNP, HGMD, and the rapidly growing local compilations) were used, when possible, to classify nucleotide differences into various categories, ranging from polymorphisms to pathogenic mutations.

Electrophysiology. The electrophysiologic properties of mutant *KCNQ1* channels were obtained by overexpression in *Xenopus laevis* oocytes as previously described (8,17,18). Experiments were performed in cells expressing WT human *KCNQ1* (NP_000209.2) and WT human *KCNE1* (NP_001121142). Mutations were generated by polymerase chain reaction–based site direct mutagenesis of the WT *KCNQ1* construct, using PFU ultra DNA polymerase and construct sequences confirmed by DNA sequencing. The average measurement of at least 18 cells expressing mutant channels were used to determine changes in ion channel parameters compared to WT channels. Thus, the same *KCNQ1* source was used for all of the mutant ion channels, with the only difference being the mutation specified in the study. All mutations analyzed for TRP were present among study subjects.

In brief, WT and mutant *KCNQ1* cRNA were injected into oocytes in a 1:1 ratio, together with the *KCNE1* subunit (0.5:0.5:1 ratio *WTKCNQ1*:*MutKCNQ1*:*KCNE1*). The IKs tail current at −40 mV was measured after depolarization to a series of voltage steps from −50 to +80 mV every 10 mV, and a Boltzmann fit ($G = g_{max}/(1 + \exp[-(V - V_{1/2})/k)$ of these data was used to determine the steepness or slope factor (k), the voltage that elicits half of the maximal activation ($V_{1/2}$) of activation, and the maximal conductance (g_{max}). Nonsense mutation effects were assumed to have had a haploinsufficient phenotype, and effects were evaluated by measuring currents with decreased WT expression (0.5:1 ratio *WTKCNQ1*:*KCNE1*).

Statistics. Linear regression was used to test for correlation between simulated repolarization time using the model described above and QTc measured from patients. Kaplan-Meier survival analysis was used to determine the cumulative probability of cardiac events by simulated repolarization

JACC Vol. 60, No. 21, 2012
November 20/27, 2012:2182–91

times and by measured QTc interval, and significance was tested by the log-rank test. Multivariate Cox proportional hazards regression modeling was used to evaluate the independent contribution of simulated repolarization times to the occurrence of cardiac events from birth through age 40 years. Additional prespecified covariates in the multivariate models included sex, the patient's individual QTc, and time-dependent beta-blocker therapy (i.e., by taking into account in the multivariate model's information regarding administration of beta-blockers given to patients at different time points during follow-up). Patients who did not have an ECG for QTc measurement (n = 92) were identified in the Cox models as "QTc missing," and all Cox models were adjusted for this missing QTc parameter. Data from the International LQTS Registry demonstrated that an age-interaction existed regarding the effect of sex and genotype on the occurrence of cardiac events, with a crossover effect for both genotype and sex after the onset of adolescence (5,19). During childhood, the risk for cardiac events is significant higher in boys with LQTS, in particular LQT1 (5,19–21). Therefore, to avoid a violation of the proportional-hazards assumption, models were carried out using a time-dependent covariate for sex with prespecified younger males (ages 0 through 13 years) and older females (ages 14 through 40 years), allowing for different hazard ratios by sex before and after adolescence.

Because almost all of the patients were first- and second-degree relatives of probands, the effect of lack of independence between patients was evaluated in the Cox model, with grouped jackknife estimates for family membership (9). All grouped jackknife standard errors for the covariate risk factors fell within 3% of those obtained from the unadjusted Cox model, and therefore only the Cox model findings are reported. The statistical software used for the analyses was SAS version 9.20 (SAS Institute Inc., Cary, North Carolina). A 2-sided 0.05 significance level was used for hypothesis testing.

Results

Simulation of transmural repolarization time. Simulation of transmural ECGs was performed for each of the mutants using mutant basic electrophysiological characteristics as previously determined (8), producing the simulated transmural electrical potentials shown in Figures 1A and 1B. The change in simulated transmural repolarization time for mutant channels compared to WT is referred to as the *TRP*. *Transmural repolarization* was defined as the difference of WT and mutant pseudo-transmural QT measured at the end of the T wave. The maximal slope intercept method was used, defining the end of the T wave as the intercept between the isoelectric line with the tangent drawn through the maximum down slope of the T wave (Fig. 1C). TRP values associated with each mutant channel are shown in Figures 1A and 1D. For one of the mutant channels tested (*D611Y*), repolarization time was predicted to be shorter (−7 ms) than the one produced by the presence of the WT channel, while other mutations caused changes ranging from +4 ms (*R591H*) to +49 ms (*G314S*). The mean TRP for all mutations was 27.5 ms. Mutations with the largest effects on TRP (top quartile [>36 ms]) were present in the transmembrane domain of the channel—1 in the S4-S5 cytoplasmic loop (*V254M*), 1 in the S5 membrane spanning domain (*L266P*), and 2 in the pore loop (*T312I* and *G314S*). Figure 1E shows the KCNQ1 channel protein with the location of the mutations in the study population. Mutations resulting in TRP in the top quartile are shown in red, and others are shown in green.

Table 1 Characteristics of the Study Population

Characteristic	TRP		p Value
	Upper Quartile (n = 186)	Lower Quartiles (n = 447)	
ECG parameters			
Overall QTc, ms	502 ± 53	475 ± 49	<0.001
QTc >500 ms	49	26	<0.001
RR, ms	804 ± 232	847 ± 200	0.04
LQTS therapies during follow-up			
Beta blockers	47	44	0.49
Pacemaker	1.1	2.2	0.49
ICD	6	8	0.39
Cardiac events during follow-up			
Syncope	59	29	<0.001
ACA, %	7	2	0.007
SCD	18	7	<0.001
Appropriate ICD shocks	0	0.2	
ACA or SCD*	23	9	<0.001
Race			
Caucasian	69.5	80	<0.001
Asian	2	12	<0.001
Other	0.5	0	
Unknown†	28	8	<0.001

Values are mean ± SD or %. *Only the first event for each patient was considered. †Patients of unknown race from Northern European Registries, likely Caucasian.

ACA = aborted cardiac arrest; ICD = implantable cardioverter defibrillator; LCSD = left cervical sympathetic denervation; MS = membrane spanning domain; SCD = sudden cardiac death.

Baseline patient characteristics by TRP. A simulated value of prolonged transmural repolarization (TRP upper quartile) among all mutations studied was present in 186 patients (29%). The mean QTc of these patients was 502 ± 53 ms, significantly prolonged compared to patients with a simulated lower quartiles TRP (475 ± 49 ms; $p < 0.001$). Other baseline characteristics of patients with upper quartile TRP are shown in Table 1, demonstrating no significant difference in heart rate (RR interval), sex, or beta-blocker usage among patients with a prolonged TRP. In addition, patients with upper quartile TRP had a higher frequency of cardiac events during follow-up, including syncope, ACA, and SCD (Table 1).

Correlation between TRP and measured QTc. To measure the correlation between TRP and individual patient QTc, TRP for each patient was plotted against the patients' measured baseline QTc (Fig. 1D). This plot illustrates the

broad variation in QTc measurements from patients with the same mutation. Simple linear regression (shown as red solid line), demonstrates a weak association between QTc and TRP ($R = 0.27$; $p < 0.0001$). Although the values were correlated, there was a wide distribution of individual QTcs for each modeled mutation. The baseline QTc measurements variation among patients with the same IKs mutation also was consistent with the significant variation observed among multiple measurements taken from a single individual (7). The correlation coefficient (R^2) for a linear correlation between individual QTc for all patients and mean QTc for patients with each mutation was 0.11 (Online Fig. 4A), suggesting that QTc variability among individuals shows, as TRP, a weak correlation with QTc variability. These results suggest that modeled TRP values predicted the ion channel mutation–specific contribution of cardiac risk. Consistent with TRP explaining a population variability of QTc, TRP showed a reasonable correlation with the mean QTc in a population with the same mutation (TRP vs. mean QTc for all patients with each mutation; $R^2 = 0.35$) (Online Fig. 4B). In addition, to estimate individual QTc variability, data from 10 patients in whom a large number of QTc determinations was available were examined (these data were not included in the primary study). These patients showed an average QTc standard deviation of (39 ± 1 ms) (Online Fig. 5), similar to that found among patients with the same mutation (39 ± 2 ms) (Online Fig. 5), suggesting that QTc variability may reflect, in large, variability observed in the individual patient over time. Because of this inherent variability in QTc determination, deterministic modeling results, such as TRP, may provide a clearer signal that can be used to evaluate risk in the patient.

TRP is an independent risk factor for cardiac events in LQT1. In a multivariate Cox regression model, mutant-specific TRP was significantly associated with an increased rate of cardiac events both as a continuous and as a dichotomized variable independent from other clinical variables and after adjustment for the patient's individual QTc (Table 2). For every additional 10-ms increment in simulated TRP, there was a corresponding significant 35% ($p < 0.001$) increase risk for the occurrence of cardiac events. Kaplan-Meier survival analysis with 4 subclassifications of TRP showed that the top quartile of TRP has an increased cumulative probability of cardiac events compared to those of the 3 lower quartiles (Online Fig. 6), indicating that probability of cardiac events is associated with a threshold level of TRP. In patients with mutations identified to have upper quartile with a simulated TRP, the risk for cardiac events was increased nearly 3-fold ($p < 0.001$). Consistent with these findings, Kaplan-Meier survival analysis (Fig. 2A, middle panel) showed that the cumulative probability of cardiac events from birth through age 40 years was significantly higher among patients with upper quartile simulated TRP compared with patients with lower TRP values. The population in the International Long QT Registry is estimated to be approximately 90% Caucasian.

Table 2 Multivariate Analysis: Risk Factors for Cardiac Events (Syncope, Sudden Death, and Aborted Cardiac Arrest) Among Patients With LQT1*

Parameter	Hazard Ratio	95% CI	p Value
TRP assessed as a continuous measure			
TRP per 10 ms	1.35	1.18–1.56	<0.001
QTc ≥500 ms vs. <500 ms	1.78	1.34–2.38	<0.001
Male age ≤13 years	1.58	1.16–2.14	0.003
Female age ≥14 years	1.47	0.98–2.19	0.06
Time-dependent β-blocker	0.37	0.20–0.66	<0.001
TRP dichotomized at the upper quartile			
TRP Q4 vs. Q1–3	2.80	1.96–4.01	<0.001
QTc ≥500 ms vs. <500 ms	1.78	1.37–2.32	<0.001
Male age ≤13 years	1.60	1.19–2.15	0.002
Female age ≥14 years	1.38	0.91–2.09	0.13
Time dependent β-blocker	0.32	0.18–0.58	<0.001

*Multivariate analysis was carried out using Cox proportional hazards regression modeling; separate models were developed for each analysis, with adjustments for the 5 covariates in each part.

LQT1 = long QT syndrome type 1; QTc = QT interval corrected for heart rate; TRP = simulated pseudo-transmural electrocardiographic prolongation.

Asian race is underrepresented in the high quartile TRP (Table 1); nonetheless, when race was included in the models, it did not predict outcome, and the effect of TRP was similar.

Simulation of transmural ECG prolongation as an independent risk factor for cardiac events in LQT1 in patient with QTc <500 ms. In a secondary analysis, risk factors for cardiac events were evaluated among patients with only mild to moderate QTc prolongation (<500 ms) because, in this patient subset, individual QTc provides less prognostic information. Among these patients, each additional 10 ms of simulated TRP was associated with a significant 36% ($p < 0.001$) increased risk for cardiac events (Table 3). Upper quartile TRP was associated with nearly a 3-fold increased risk (2.97; 95% CI: 2.00 to 4.40) after adjustment for patients' individual QTc. Consistent with these findings, Kaplan-Meier curves including only patients with QTc <500 ms demonstrated early separation of event-free survival rates when patients were grouped into the upper versus lower TRP quartiles (Fig. 2B). When patients were stratified by both individual baseline QTc and TRP, Kaplan-Meier survival analysis showed that the group with upper TRP had a significantly higher event rate throughout follow-up, regardless of patients' individual QTc (Fig. 2C). Results from multivariate Cox proportional hazard regression analysis corresponding to the groups in Figure 2C are shown in Online Table 2.

To test whether TRP simulation parameters further improved clinical risk stratification compared with previously identified risk factors related to ion channel characteristics, secondary analysis added slow rate of channel activation as a covariate. Previous work showed that that channels with slow rates of activation (over 20% slower than WT channels) were associated with an increased risk for cardiac events (8). The results showed that for both the

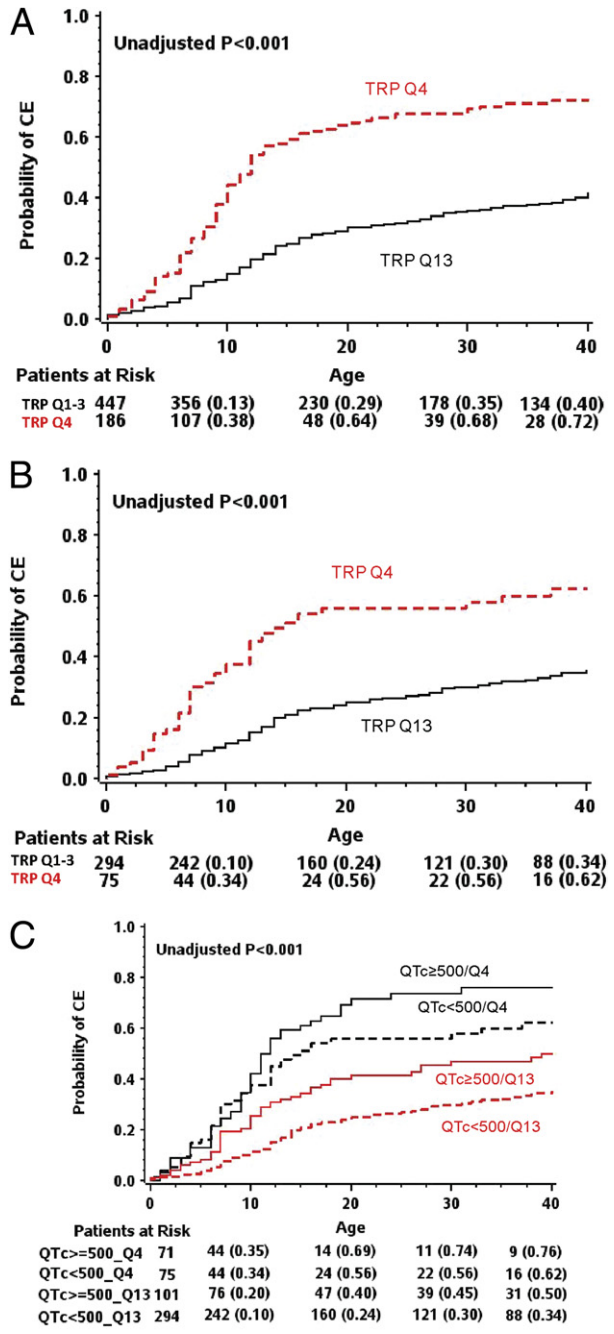

Figure 2 Rate of Cardiac Event During Follow-Up

Cumulative probability of the first cardiac event (syncope, aborted cardiac arrest, or death) during follow-up, dichotomized by patients with the highest quartile TRP (Q4) and all other quartiles (Q1–3) **(A)** among all study patients; **(B)** among the subset of patients with QTc <500 ms; **(C)** among all patients with combined assessment of TRP and QTc. Abbreviations as in Figure 1.

population as a whole and for patients with QTc <500 ms, slower channel activation and TRP top quartile were independent risk factors (Table 3). Additionally, because QTc ≥480 ms was found to be a very poor predictor of event risk in this population (hazard ratio [HR]: 0.96; 95% CI: 0.63 to 1.46; p = 0.85), a secondary analysis evaluated the association between QTc ≥450 ms and event risk in this population. This lower threshold was a similarly poor predictor of risk (HR: 1.09; 95% CI: 0.71 to 1.67; p = 0.71) (Online Table 3).

Simulation of transmural ECG prolongation as an independent risk factor for life-threatening cardiac events (ACA/SCD) in LQT1. In a multivariate Cox regression model, mutation-specific TRP was also significantly associated with an increased risk for live-threatening cardiac events (defined as first occurrence of ACA or SCD). The risk for ACA/SCD associated with TRP was consistent when this parameter was assessed as both a continuous measure and dichotomized at the upper quartile (>36 ms), after adjustment for individual patients' QTc (Table 4). Thus, for every additional 10 ms of added simulated transmural repolarization time, there was a corresponding significant 37% increase in the risk for ACA/SCD. Furthermore, the group carrying a mutation with upper quartile TRP had a >2-fold (p = 0.002) increased risk for ACA/SCD after adjustment for the individual patients' QTc (Table 5). This is also illustrated by Kaplan-Meier curves (Fig. 3), with early separation of event-free survival rates for the population of patients with upper quartile TRP.

Discussion

This study describes a method of simulating transmural myocardial repolarization based on WT and mutant channel characteristics determined in cellular electrophysiology. This transmural repolarization parameter was found to be an independent predictor for the occurrence of cardiac events and life-threatening events in patients with LQT1. The risk associated with simulated TRP was shown to be independent of patients' baseline QTc. These results regarding mutation-specific risk are particularly important for the subpopulation with mild to moderate QTc prolongation

Table 3 Multivariate Analysis: Risk Factors for Cardiac Events (Syncope, Sudden Death and Aborted Cardiac Arrest) Among 369 patients with LQT1 and QTc <500 ms

Parameter	Hazard Ratio	95% CI	p Value
TRP assessed as a continuous measure			
TRP per 10 ms	1.36	1.18–1.56	<0.001
QTc ≥480 ms vs. <480 ms	0.99	0.67–1.46	0.97
Male aged ≤13 years	1.42	0.87–2.33	0.16
Female aged ≥14 years	1.86	0.96–3.60	0.06
Time-dependent β-blocker	0.48	0.23–1.02	0.06
TRP dichotomized at the upper quartile			
TRP Q4 vs. Q1–3	2.97	2.00–4.40	<0.001
QTc ≥480 ms vs. <480 ms	0.96	0.63–1.46	0.85
Male aged ≤13 years	1.38	0.86–2.21	0.19
Female aged ≥14 years	1.90	0.98–3.67	0.06
Time dependent β-blocker	0.45	0.22–0.58	0.04

Abbreviations as in Table 2.

Table 4 Multivariate Analysis: Risk Factors for Cardiac Events (Syncope, Sudden Death and Aborted Cardiac Arrest)*

Parameter	Hazard Ratio	95% CI	p Value
TRP dichotomized at the upper quartile for the whole population			
TRP Q4 vs. Q1–3	2.25	1.49–3.39	<0.001
τ_{act} >1.20	1.42	1.00–2.03	0.05
QTc ≥500 ms vs. <500 ms	1.73	1.32–2.27	<0.001
Male aged ≤13 years	1.60	1.17–2.18	0.003
Female aged ≥14 years	1.39	0.981–2.11	0.12
Time dependent β-blocker	0.33	0.18–0.59	<0.001
TRP dichotomized at the upper quartile for patients with QTc <500 ms			
TRP Q4 vs. Q1–3	2.11	1.23–3.61	<0.01
τ_{act} >1.20	1.70	1.03–2.80	0.04
QTc ≥480 ms vs. <480 ms	0.94	0.62–1.43	0.78
Male aged ≤13 years	1.39	0.84–2.28	0.19
Female aged ≥14 years	1.86	0.95–3.65	0.07
Time dependent β-blocker	0.44	0.21–0.92	0.03

*Multivariate analysis was carried out using Cox proportional hazards regression modeling; separate models were developed for each analysis, with adjustments for the covariates in each part.
Abbreviations as in Table 2.

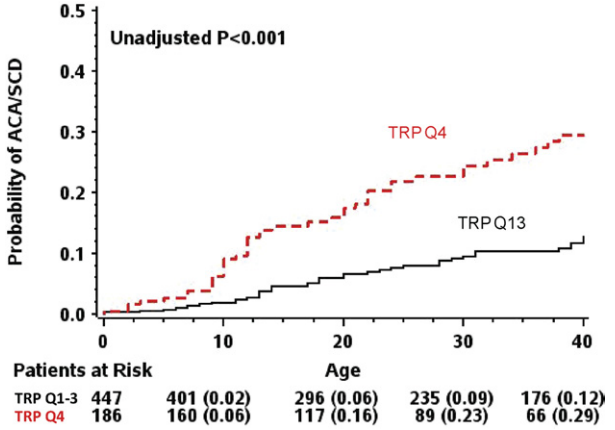

Figure 3 Rates of Life-Threatening Cardiac Events During Follow-Up

Cumulative probability of aborted cardiac arrest or sudden cardiac death during follow-up among all study patients, dichotomized by patients with the highest quartile TRP (Q4) and all other quartiles (Q1–3). Abbreviations as in Figure 1.

(QTc <500 ms), in whom clinical risk factors provide less prognostic value. This report shows cardiac modeling being used as an arrhythmic risk predictor validated against a patient population in clinical practice.

Several experimental and computation models have been developed on the premise that transmural ECGs are a surrogate for the QT interval as measured by body surface ECGs. Transmural repolarizations are also thought to be particularly important in generating inhomogeneities of repolarization that lead to cardiac arrhythmias (22,23). IKs channel expression changes across the ventricular wall, contributing to transmural dispersion of repolarization (24–26). This is consistent with the present results, which indicate a significant increase in cardiac risk associated with mutation-specific changes in IKs and transmural repolarization in LQT1. In these models, the action potential duration dispersion can produce conditions to support reentrant activation patterns. Future, more detailed studies of arrhythmia mechanisms modeling higher dimensional tissue structure that can support a reentrant activation pattern are necessary. In addition, the use of TRP as an index for cardiac risk in other inherited and acquired LQT syndromes is promising but needs further study.

Table 5 Multivariate Analysis: Risk Factors for SCD/ACA Among All Patients With LQT1*

Parameter	Hazard Ratio	95% CI	p Value
TRP used as a continuous variable			
TRP per 10-ms increment	1.27	1.02–1.59	0.03
QTc ≥500 ms	3.93	1.96–7.87	<0.001
Male age ≤13 years	2.16	1.22–3.84	0.008
Female age ≥14 years	1.19	0.63–2.26	0.59
Time dependent β-blocker	0.40	0.16–0.98	0.046
TRP dichotomized at top quartile			
TRP Q4 vs. Q1–3	2.24	1.96–4.01	0.002
QTc ≥500 ms vs. <500 ms	3.95	1.37–2.32	<0.001
Male age ≤13 years	2.24	1.19–2.15	0.005
Female age ≥14 years	1.12	0.91–2.09	0.74
Time dependent β-blocker	0.38	0.15–0.94	0.04

*Multivariate analysis was carried out using Cox proportional hazards regression modeling; separate models were developed for each analysis, adjusting for the 5 covariates in each part.
Abbreviations as in Table 2.

The authors showed previously that a slow activation rate is an independent risk factor in LQT1. The results indicate that TRP is independent from channel slow activation rate. Notable is that all 4 mutant channels in the top quartile of TRP show also slow activation kinetics (8). Nonetheless, TRP combines slower activation, changes in voltage dependence of activation, and conductance of the channel in relevant cardiac cell types to provide an overall effect of the mutation regarding transmural repolarization. This utilizes information on ion channel distribution and consequences of ion channel dysfunction for APD and propagation across the myocardial wall. Using this novel method, 4 high-risk mutations were identified, only 1 of which had been identified in the previous study. Most important, the present study showed that these high-risk mutations predicted life-threatening arrhythmic risk in the study population.

The simulation model proposed here consists of electrically coupled cardiac cells with heterogeneous electrophysiologic properties that produce waveforms that are similar to those measured experimentally (27–29). The development of heterogeneous models depends both on accurately representing the AP of the different cell populations and realistic coupling between the cells. At the single cell level, the exact difference in membrane currents and Ca^{2+} handling that produce differences across the ventricular wall is

controversial and very likely both region and species dependent. On the basis of the 3 standard cell types (epi-, endo-, and midmyocardial) in Flaim et al. (14), parameters were continually varied to interpolate differences in IKs, transient outward potassium current (I_{to}), I_{NaL}, and Ca^{2+} handling in an attempt to match the experimentally measured transmural profiles (28). The conductivity between cells was assumed to have been fixed, so that the conduction velocity was constant across the ventricular wall, as seen experimentally (28,30). This assumption of constant conductivity is consistent with the limited available experimental data that show that resistance is uniform, with the exception of a layer with higher resistivity (29). This layer, situated to roughly 30% depth, involves a systematic change in cellular orientation. The discontinuity in cellular orientation cannot be directly represented in the 192 equally spaced point models comprising our 1-D cable. However, future extensions to the model could incorporate this additional level of detail.

A recent study (31) used Markov models, AP and transmural ECG simulations to infer the mechanism of arrhythmia generation associated with a LQT1 associated mutation present in 1 patient with normal QTc and a history of syncope (*Q357R,* not included in the present study). The predisposition to arrhythmia was demonstrated by the propensity to generate early after depolarization (EADs) when combined with IKr blockage and beta-adrenergic drive, whereas the effect on the simulated TRP alone (without IKr blockage and beta-adrenergic drive) was mild (13 ms). This TRP value is comparable to the ones associated with mutations in this study with TRP in the first quartile, a range associated with 35% risk for a cardiac event by age 40 years. In contrast to the previous study, the present study focuses on how TRP relates to a clinical risk that may be revealed over the time frame of up to 40 years for a patient population. Because the present study included a large number of mutations, we chose a simpler Hodgkin-Huxley model of IKs that could be systematically constrained by the in vitro data. Although Markov models can potentially capture additional mechanistic details of ion channel function, identification of states and constraining parameters are difficult and complex with typical electrophysiologic data (32).

Simulated repolarization prolongation weakly correlated with baseline QTc measurements in the study population, which supports physiologic relevance of the simulation method. However, QTc measurements can vary widely among patients with a particular mutation and over time in the same patient (7). In addition, QTc has been shown to change during exercise (33) and with age (5) and has been suggested to depend on a patient's emotional state (34). The simulated transmural repolarization parameter described here may reflect an overall lifetime risk in patients with each specific mutation, a risk that may not be reflected in a single determination of patients' QTc. A reasonable correlation was found between the TRP and the mean QTc in a population with the same genotype, suggesting that deterministic modeling results may provide a clearer signal than patient data with high variability and stochastic effects. Other genetic factors (e.g., SNPs in ion channels, modifier protein, and receptors) and unknown functional effect of the mutations, such as a decrease in beta-adrenergic activation (35), that are not taken into account in the TRP modeling, may also influence individual patients' QTc and/or risk for cardiac arrhythmias, with the possibility of both influencing or masking genotype-specific cardiac risk.

Here, mutations associated with high risk for cardiac events were identified in patients with LQT1. Four of these mutations, the ones included in the top quartile of repolarization dysfunction, were identified as being of particularly high risk: *V254M, L266P, T312I,* and *G314S*. These are all highly conserved residues among voltage-gated potassium channels, suggesting an important physiologic role (8,36). The authors recently showed that *V254M* has impaired beta-adrenergic activation, which would contribute to an increase in risk in patients with this mutation at high adrenergic states; the other mutations were not identified previously as being of particularly high risk.

Study limitations. Although the present findings regarding the use of simulated TRP in risk stratification are novel, these results are based on a single-population study of 633 patients with LQT1, and therefore need to be further validated in larger populations, comprising also patients with recently identified novel mutations in the *KCNQ1* gene. Partly retrospective data collection has limitations. However, because this is an analysis of registry data of a rare disease (in which a prospective clinical trial or an analysis of events from birth would be difficult), the authors believe that this type of analysis is the best way to handle the survival bias conferred by entering the registry at an older age and the exclusion of higher-risk patients who died at a younger age. The present study attempted to identify the incremental prognostic implications of computed modeling of electrophysiologic modeling in LQTS, but did not investigate the reason why the model TRP is a good risk predictor. For this, higher-dimensional tissue structure that can support a re-entrant activation pattern is necessary.

Conclusions

The identification of mutations conferring a high risk for cardiac events can help to guide treatment decisions by identifying those patients who will benefit most from therapies including pharmacologic agents (i.e., beta-blockers) and implantable defibrillators. In particular, patients with moderate QTc prolongation (i.e., QTc <500 ms) are a challenge for clinicians because their risk for cardiac events remains significantly elevated compared to that of the general population, although the markers of risk are relatively unknown (9). We have shown that simulated TRP is a particularly strong marker of risk for cardiac events in this population, which may translate into changes in treatment decisions for identifying high-risk LQTS patients

independently of traditional ECG markers. It would be recommended that patients with the identified prolonged TRP mutations (*V254M, G314S, T312I,* and *L266P*) should be considered to be at a high risk for cardiac events even in the absence of QTc prolongation or other clinical risk factors. This patient subset should be routinely treated with beta-blocker therapy at the maximal tolerated dosage and carefully followed up for residual symptoms during medical therapy.

Reprint requests and correspondence: Dr. Coeli M. Lopes, Department of Medicine, Box CVRI, Aab Cardiovascular Research Institute, University of Rochester School of Medicine & Dentistry, 601 Elmwood Avenue, Rochester, New York 14642. E-mail: Coeli_Lopes@URMC.Rochester.edu OR Dr. Ilan Goldenberg, Heart Research Follow-up Program, Box 653, University of Rochester Medical Center, Rochester, New York 14642. E-mail: Ilan.Goldenberg@heart.rochester.edu.

REFERENCES

1. Keating MT, Sanguinetti MC. Molecular and cellular mechanisms of cardiac arrhythmias. Cell 2001;104:569–80.
2. Hedley PL, Jorgensen P, Schlamowitz S, et al. The genetic basis of long QT and short QT syndromes: a mutation update. Hum Mutat 2009;30:1486–511.
3. Moss AJ. Long QT syndrome. JAMA 2003;289:2041–4.
4. Moss AJ, Shimizu W, Wilde AAM, et al. Clinical aspects of type-1 long-QT syndrome by location, coding type, and biophysical function of mutations involving the KCNQ1 gene. Circulation 2007;115:2481–9.
5. Zareba W, Moss AJ, Locati EH, et al. Modulating effects of age and gender on the clinical course of long QT syndrome by genotype. J Am Coll Cardiol 2003;42:103–9.
6. Priori SG, Napolitano C, Schwartz PJ, et al. Association of long QT syndrome loci and cardiac events among patients treated with beta-blockers. JAMA 2004;292:1341–4.
7. Goldenberg I, Mathew J, Moss AJ, et al. Corrected QT variability in serial electrocardiograms in long QT syndrome: the importance of the maximum corrected QT for risk stratification. J Am Coll Cardiol 2006;48:1047–52.
8. Jons C, Uchi J, Moss AJ, et al. Use of mutant-specific ion channel characteristics for risk stratification of long QT syndrome patients. Sci Transl Med 2011;3:76ra28.
9. Goldenberg I, Horr S, Moss AJ, et al. Risk for life-threatening cardiac events in patients with genotype-confirmed long-QT syndrome and normal-range corrected QT intervals. J Am Coll Cardiol 2011;57:51–9.
10. Horr S, Goldenberg I, Moss AJ, et al. Ion channel mechanisms related to sudden cardiac death in phenotype-negative long-QT syndrome genotype-phenotype correlations of the KCNQ1(S349W) mutation. J Cardiovasc Electrophysiol 2011;22:193–200.
11. Bianchi L, Priori SG, Napolitano C, et al. Mechanisms of I-Ks suppression in LQT1 mutants Am J Physiology-Heart Circ Physiol 2000;279:H3003–11.
12. Murray A, Potet F, Bellocq C, et al. Mutation in KCNQ1 that has both recessive and dominant characteristics. J Med Genet 2002;39:681–5.
13. Wang Z, Tristani-Firouzi M, Xu Q, Lin M, Keating MT, Sanguinetti MC. Functional effects of mutations in KvLQT1 that cause long QT syndrome. J Cardiovasc Electrophysiol 1999;10:817–26.
14. Flaim SN, Giles WR, McCulloch AD. Contributions of sustained I-Na and I-Kv43 to transmural heterogeneity of early repolarization and arrhythmogenesis in canine left ventricular myocytes. Am J Physiol-Heart Circ Physiol 2006;291:H2617–29.
15. Narayan SM, Bayer JD, Lalani G, Trayanova NA. Action potential dynamics explain arrhythmic vulnerability in human heart failure. J Am Coll Cardiol 2008;52:1782–92.
16. Keller DU, Seemann G, Weiss DL, Farina D, Zehelein J, Dossel O. Computer based modeling of the congenital long-QT 2 syndrome in the Visible Man torso: from genes to ECG. Conf Proc IEEE Eng Med Biol Soc 2007;1410–3.
17. Matavel A, Lopes CMB. PKC activation and PIP2 depletion underlie biphasic regulation of IKs by Gq-coupled receptors. J Mol Cell Cardiol 2009;46:704–12.
18. Matavel A, Medei E, Lopes CM. PKA and PKC partially rescue long QT type 1 phenotype by restoring channel-PIP2 interactions. Channels (Austin) 2010;4:3–11.
19. Locati EH, Zareba W, Moss AJ, et al. Age- and sex-related differences in clinical manifestations in patients with congenital long-QT syndrome—Findings from the international LQTS registry 11. Circulation 1998;97:2237–44.
20. Goldenberg I, Moss AJ, Peterson DR, et al. Risk factors for aborted cardiac arrest and sudden cardiac death in children with the congenital long-QT syndrome. Circulation 2008;117:2184–91.
21. Hobbs JB, Peterson DR, Moss AJ, et al. Risk of aborted cardiac arrest or sudden cardiac death during adolescence in the long-QT syndrome. JAMA 2006;296:1249–54.
22. Antzelevitch C, Shimizu W. Cellular mechanisms underlying the long QT syndrome. Curr Opin Cardiol 2002;17:43–51.
23. Antzelevitch C, Shimizu W, Yan GX, Sicouri S. Cellular basis for QT dispersion. J Electrocardiol 1998;30 Suppl:168–75.
24. Pajouh M, Wilson LD, Poelzing S, Johnson NJ, Rosenbaum DS. IKs blockade reduces dispersion of repolarization in heart failure. Heart Rhythm 2005;2:731–8.
25. Shimizu W, Antzelevitch C. Cellular basis for the ECG features of the LQT1 form of the long-QT syndrome: effects of beta-adrenergic agonists and antagonists and sodium channel blockers on transmural dispersion of repolarization and torsade de pointes. Circulation 1998;98:2314–22.
26. Antzelevitch C, Sun ZQ, Zhang ZQ, Yan GX. Cellular and ionic mechanisms underlying erythromycin-induced long QT intervals and torsade de pointes. J Am Coll Cardiol 1996;28:1836–48.
27. Zhu TG, Patel C, Martin S, et al. Ventricular transmural repolarization sequence: its relationship with ventricular relaxation and role in ventricular diastolic function. Eur Heart J 2009;30:372–80.
28. Yan GX, Antzelevitch C. Cellular basis for the normal T wave and the electrocardiographic manifestations of the long-QT syndrome. Circulation 1998;98:1928–36.
29. Yan GX, Shimizu W, Antzelevitch C. Characteristics and distribution of M cells in arterially perfused canine left ventricular wedge preparations. Circulation 1998;98:1921–7.
30. Zhu TG, Patel C, Martin S, et al. Ventricular transmural repolarization sequence: its relationship with ventricular relaxation and role in ventricular diastolic function. Eur Heart J 2009;30:372–80.
31. O'Hara T, Virag L, Varro A, Rudy Y. Simulation of the undiseased human cardiac ventricular action potential: model formulation and experimental validation. PLoS Comput Biol 2011;7:e1002061.
32. Fink M, Noble D. Markov models for ion channels: versatility versus identifiability and speed. Philos Transact A Math Phys Eng Sci 2009;367:2161–79.
33. Vincent GM, Jaiswal D, Timothy KW. Effects of exercise on heart rate, QT, QTc and QT/QS2 in the Romano-Ward inherited long QT syndrome. Am J Cardiol 1991;68:498–503.
34. Lane RD, Carmichael C, Reis HT. Differentiation in the momentary rating of somatic symptoms covaries with trait emotional awareness in patients at risk for sudden cardiac death. Psychosom Med 2011;73:185–92.
35. Barsheshet A, Goldenberg I, Uchi J, et al. Mutations in cytoplasmic loops of the KCNQ1 channel and the risk of life-threatening events: implications for mutation-specific response to beta-blocker therapy in type-1 long QT syndrome. Circulation 2012;125:1988–96.
36. Jons C, Moss AJ, Lopes CMB, et al. Mutations in conserved amino acids in the KCNQ1 channel and risk of cardiac events in type-1 Long QT syndrome. J Cardiovasc Electrophysiol 2009;20:859–65.

Key Words: IKs ■ KCNQ1 ■ KCNQ2 ■ LQT ■ QT.

APPENDIX

For a supplemental Methods section, tables, figures, and references, and additional details on the in silico methods, please see the online version of this article.